

Nanostructures of Polyaniline Doped with Inorganic Acids

Zhiming Zhang, Zhixiang Wei, and Meixiang Wan*

Organic Solid Laboratory, Center of Molecular Sciences, Institute of Chemistry, Chinese Academy of Sciences, Beijing, P. R. China 100080

Received February 6, 2002

ABSTRACT: With an average diameter of 150–340 nm and a conductivity of 10^{-1} – 10^0 S/cm, nanostructures (e.g., nanotubes or nanorods) of polyaniline (PANI) were synthesized by a self-assembly method in the presence of inorganic acids (e.g., HCl, H₂SO₄, HBF₄, and H₃PO₄) as dopants. It was found that the morphology, size, and electrical properties of the resulting nanostructures depended on the dopant structures and the reaction conditions. In particular, all these PANI nanostructures showed hydrophilic features, and the contact angles with water were measured to be about 27–40° depending on the dopant. The FTIR spectrum, UV–vis absorption spectrum, XPS, and X-ray diffraction were used to characterize the molecular structures of the nanostructures. It was found that their main chain structure and electric structure were identical to those of the emeraldine salt form of PANI. The micelles formed by anilinium cations act as the template like in the formation of PANI nanostructures.

Introduction

Studies on molecular wire have attracted more and more attention since the discovery of the first molecular wire of carbon nanotubes (CNTs);¹ thus, conducting polymers are promising in this area due to their long conjugated length and metallike conductivity.^{2,3} Nanotubes or nanofibers of conducting polymers, such as polyacetylene,⁴ poly(3-methylthiophene),⁵ polypyrrole,⁶ and polyaniline,⁷ have been synthesized by a “template synthesis” method. In our laboratory, Wan et al.⁸ reported that microtubes of polyaniline (PANI) and polypyrrole (PPy) were synthesized by in-situ doping polymerization in the presence of β -naphthalenesulfonic acid (β -NSA) as a dopant. Here, β -NSA acted as a template like in the formation of PANI-(β -NSA) microtubules due to its surfactant function (e.g., -SO₃H group). However, it was different from the “template synthesis” method. Unlike template synthesis, β -NSA did not need to be removed after polymerization because it can act as a dopant for PANI at the same time. Therefore, we call it a self-assembly method. Moreover, we have proved the reliability and practicability of this self-assembly method for synthesizing microtubes or nanotubes of conducting polymers through changing polymer chains^{9–14} and dopants^{15–17} and using different polymerization methods.¹⁸ The dopants used in our previous experiments have both doping and surfactant functions. The surfactant function of the dopant seemed to play an important role in the formation of nanostructures of conducting polymers.¹⁹ So, it is very interesting to examine whether the surfactant function of the dopant is the prerequisite to form self-assembled PANI nanostructures.

In this article, self-assembled PANI nanostructures (e.g., nanotubes or nanorods) with an average diameter of 150–340 nm and a room-temperature conductivity of 10^{-1} – 10^0 S/cm in the presence of inorganic acids (e.g., HCl, H₂SO₄, H₃PO₄, and HBF₄) as dopants are reported for the first time. The effect of the dopant structures and reaction conditions on the morphology, size, and physical properties of the resulting PANI nanostructures was investigated, and the formation mechanism of PANI nanostructures was discussed.

Experimental Section

Aniline monomer was distilled under reduced pressure. Other reagents, such as dopants (HCl, H₂SO₄, HBF₄, and H₃PO₄), oxidant (ammonium peroxydisulfate, APS), sodium dodecylbenzenesulfonate (SDBS), and hexadecyltrimethylammonium bromide (HTAB) as surfactants, were used as received.

The nanostructures of PANI doped with inorganic acids were synthesized by a self-assembly method. To understand the effect of the surfactant on the morphology of PANI, the parallel experiments with and without a surfactant were carried out. For example, PANI doped with H₃PO₄ was synthesized as follows: Aniline (0.2 mL) and SDBS (3.3 mg) were mixed with H₃PO₄ (0.06 mL) in 10 mL of deionized water in the ice bath to form a white dispersion of aniline/H₃PO₄ salt. Then an aqueous solution of APS (0.46 g in 5 mL of deionized water) was added to the above mixtures. The polymerization was carried out for 12 h in the ice bath. A green solid of PANI-H₃PO₄ was obtained after rinsing with H₂O, CH₃OH, and CH₃OCH₃ for three times. PANI-HCl, PANI-H₂SO₄, and PANI-HBF₄ were synthesized by a similar method. Meanwhile, PANI-H₃PO₄ was also synthesized without a surfactant through the same process for a comparative study.

The UV–vis spectrum, FTIR spectrum, X-ray photoelectron spectroscopy (XPS), and X-ray diffraction were used to characterize the molecular structures of the resulting PANI nanostructures. FTIR spectra were performed on a Bruker EQUINOX55, while X-ray diffraction was carried on a RINT 2000 Wilder-angle goniometer. The morphology was measured by a scanning electron microscope (SEM, Hitachi-530 or FESEM, JSM-6700F) and a transmission electron microscope (TEM, Hitachi-9000). The conductivity at room temperature was measured by a Keithley 196 SYSTEM DM digital multimeter and an ADVANTEST R6142 programmable dc voltage/current source, a standard four-probe method. XPS was performed on ES-300 (Kratos). The contact angle with water for the nanostructural film deposited on the glass substrate was measured on a contact angle system (OCA Dataphysics DCAT 11).

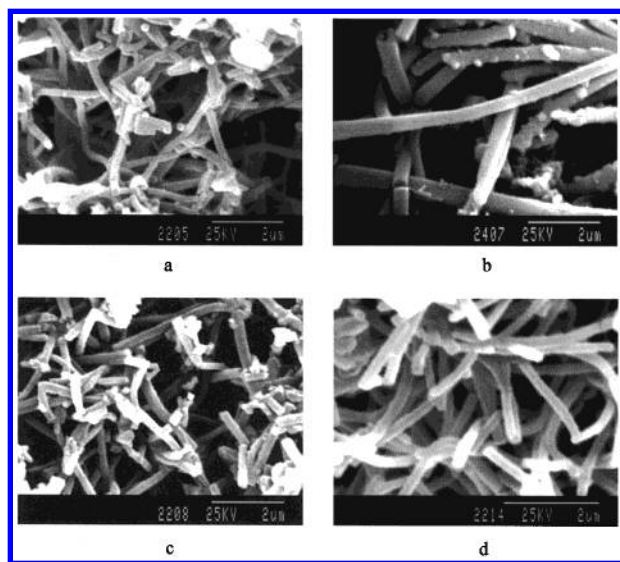
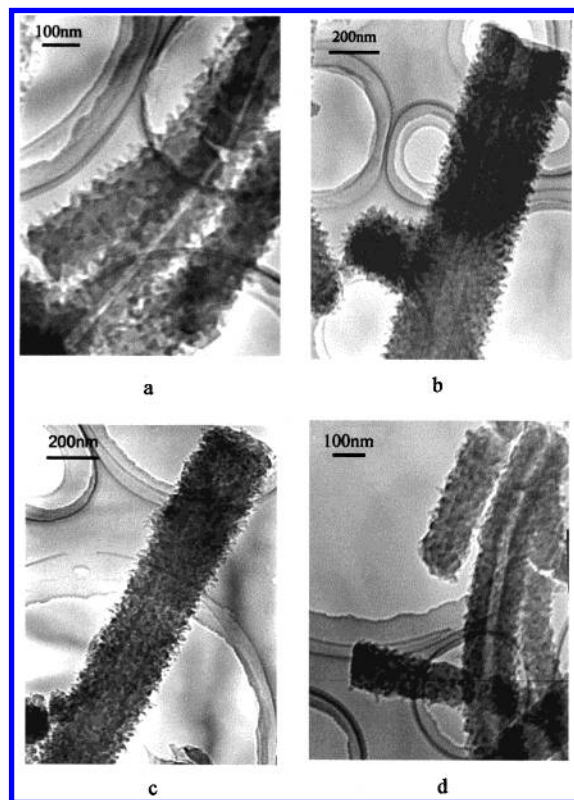
Results and Discussion

Morphologies of PANI and Their Formation Mechanism. As shown in Figure 1, all PANI samples synthesized in the presence of SDBS as a surfactant

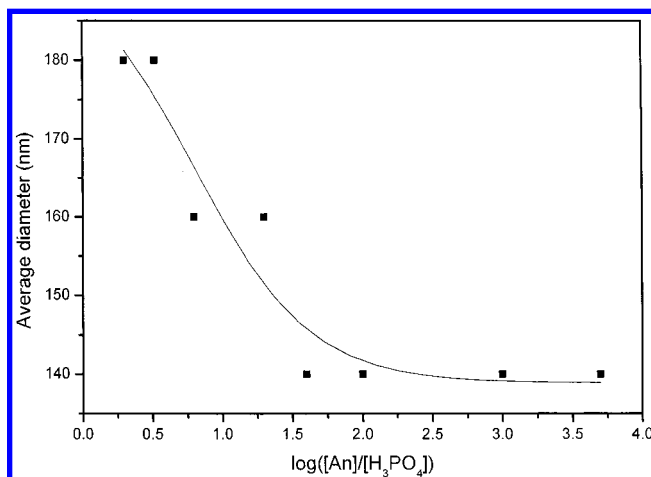
* Corresponding author: e-mail wanmx@infoc3.icas.ac.cn.

Table 1. Detailed Data of PANI Nanostructures Doped with Different Inorganic Acids

	PANI-HCl	PANI-H ₂ SO ₄	PANI-HBF ₄	PANI-H ₃ PO ₄
σ_{RT} (S/cm)	6.38	1.26	1.12	0.49
[N ⁺]/[N] (%)	13.5	14.1	14.9	18.3
average diameter (nm)	150	335	265	180
T_0 (K)	6.60×10^3	8.96×10^3	1.14×10^4	1.51×10^4
UV-vis absorption λ_{max} (nm)	423, 890	423, 881	430, 877	452, 833

**Figure 1.** SEM images of PANI nanostructures doped with different inorganic acids: (a) HCl, (b) H₂SO₄, (c) HBF₄, (d) H₃PO₄ ([An]/[acid] = 2, [SDBS] = 2.4×10^{-3} M, at 0–4 °C).**Figure 2.** TEM images of PANI nanostructures doped with different inorganic acids: (a) HCl, (b) H₂SO₄, (c) HBF₄, (d) H₃PO₄ ([An]/[acid] = 2, [SDBS] = 2.4×10^{-3} M, at 0–4 °C).

have fibrous morphology. TEM images reveal that these fibers include tubes and rods as shown in Figure 2. It was found that the size and formation probability of the nanostructures strongly depended on the dopant structure and reaction conditions (e.g., aniline/acid molar

**Figure 3.** Influence of [An]/[H₃PO₄] on the average diameter of PANI-H₃PO₄ ([SDBS] = 2.4×10^{-3} M, at 0–4 °C).

ratio and reaction temperature). For instance, the diameters of PANI nanostructures varied from 150 to 340 nm, depending on the dopant used (Table 1). The result indicates that the size of PANI nanostructures is controllable by changing the dopant structure. Moreover, the size of PANI nanostructures was affected by the aniline/acid mole ratio (represented by [An]/[acid]). Taking PANI-H₃PO₄ as an example, the average diameter of PANI-H₃PO₄ decreased slightly from 180 to 140 nm when [An]/[H₃PO₄] changed from 1:0.5 to 1:0.01. However, as shown in Figure 3, no changes took place in the average diameter of PANI-H₃PO₄ while [An]/[H₃PO₄] changed from 1:0.01 to 1:0.0002.

The formation probability of PANI nanostructures depended on reaction temperature and [An]/[acid]. It was found that the reaction temperature had an important influence on the morphology of the resulting PANI. Taking PANI-HCl as an example, besides the fibrous nanostructures, there were some granular solids when aniline was polymerized at room temperature ([An]/[acid] = 1:0.5). When the polymerization occurred at a lower temperature (0–4 °C) as mentioned above, nearly all the products showed fibrous nanostructures, and the formation probability of the nanotubes or rods was greatly enhanced. A similar result was observed when H₂SO₄ was used as the dopant. In addition, the ratio [An]/[acid] also affected the formation probability of fibrous nanostructures greatly when the polymerization was carried out at a low temperature (0–4 °C). PANI-H₃PO₄, for example, showed granular morphology when [An]/[H₃PO₄] was 1:2 or 1:3. However, some aniline/H₃PO₄ mole ratios (e.g., 1:0.5, 1:0.3, and 1:0.16) were more favorable for the formation of fibrous PANI-H₃PO₄ nanostructures. Then the formation probability of the nanostructures decreased with the increase of [An]/[H₃PO₄]. It needs to be pointed out that only a small quantity of nanostructures was obtained when [An]/[H₃PO₄] reached 1:0.0002.

The influence of the surfactant structure and concentration on the morphology of PANI nanostructures was

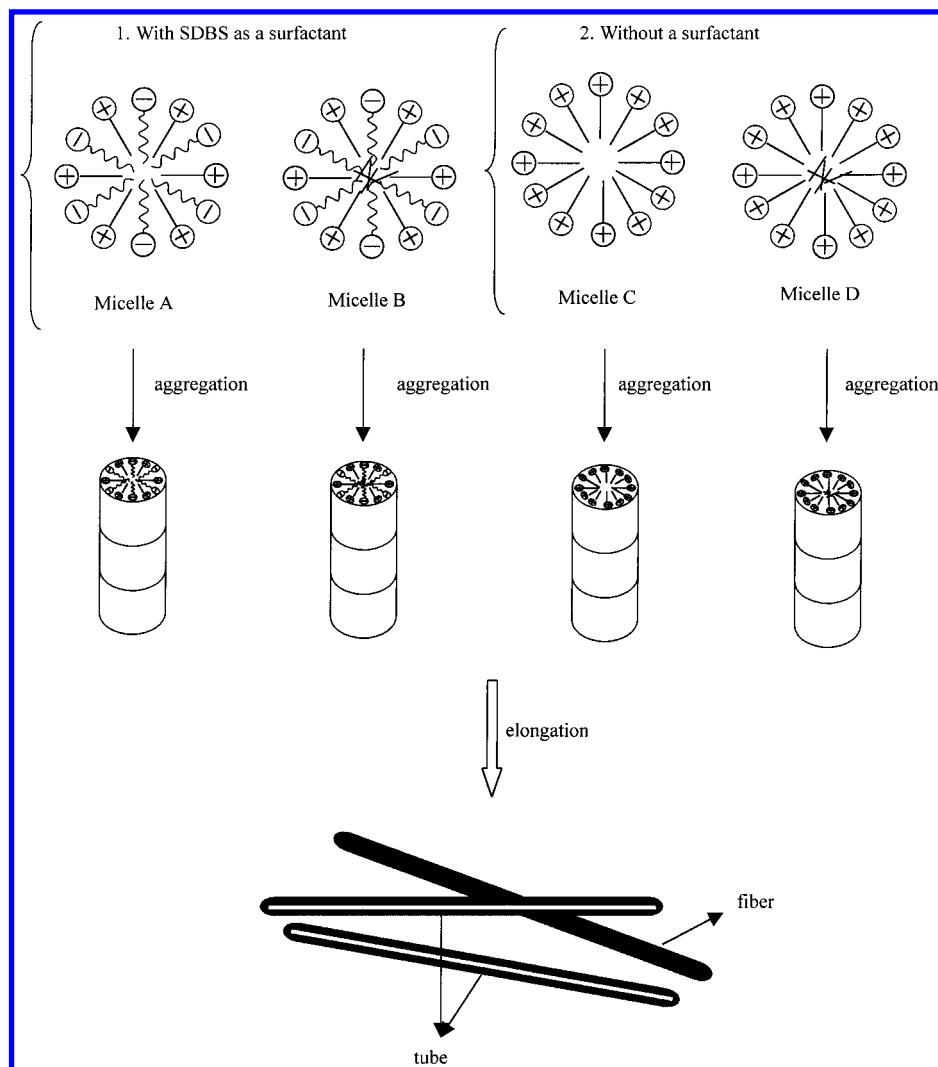


Figure 4. Schematic diagram of the formation mechanism for PANI nanostructures synthesized by a self-assembly process.

investigated in order to examine whether the surfactant is the prerequisite to form self-assembled PANI nanostructures. It was found that PANI- H_3PO_4 had the same diameter (~ 180 nm) when the concentration of SDBS changed from 2.4×10^{-3} to 1.3×10^{-2} M, showing the concentration of SDBS had little effect on the morphology and size of PANI- H_3PO_4 nanostructures. When using HTAB instead of SDBS as the surfactant, the average diameter of PANI- H_3PO_4 nanostructures only varied from 180 to 200 nm with the concentration of HTAB changing from 8.0×10^{-3} to 1.6×10^{-2} M. And then the diameter kept constant even when the concentration of HTAB increased to 5×10^{-2} M. This result is consistent with that of PANI- H_3PO_4 synthesized in the presence of SDBS as a surfactant. PANI- H_3PO_4 nanostructures, with their diameter of 150 nm, were also obtained even though no surfactant was added. Thus, the above results indicate that surfactant function of the dopant is not the prerequisite for the formation of self-assembled PANI nanostructures. However, the addition of the surfactant and its concentration do affect the size of PANI nanostructures.

How does one interpret the formation of PANI nanostructures by a self-assembly process?

If SDBS is used as the surfactant (represented by $\odot\sim$), it is easy to form micelles. At the same time, aniline may exist in the form of anilinium salt (represented by $\oplus-$) or free aniline (represented by

in the reaction solution. Spherical micelles as templates may be formed.²⁰ Anilinium cations can be solubilized in the micelle-water interface to form micelle A, or a part of free aniline diffuses into micelles to form micelle B²¹ as shown in Figure 4. Micelles A and B are assumed as the templates to form PANI nanostructures in the presence of a surfactant. On the other hand, it is expected that micelles C and D (Figure 4) formed by anilinium cations might be the templates to form PANI nanostructures in the absence of a surfactant. Solubilized aniline or anilinium molecules are polymerized oxidatively by APS existing in the aqueous phase. The reaction takes place mainly in the micelle-water interface adjacent to the surfactant headgroups because hydrated APS molecules cannot penetrate into the micelle surface.²² With the polymerization proceeding, the micelles become big spheres through accretion²³ or tubes/rods through elongation²⁴ depending on the local conditions. In our experiments, it is obvious that the occurrence of the elongation procedure judges from the morphology of the resulting PANI. Then micelles A or C will be converted into tubes and micelles B or D into rods. The size of the micelles may greatly affect the size of the resulting nanostructures; therefore, PANI samples doped with different inorganic acids have different diameters. Up to now, it is reasonable to conclude that PANI nanostructures doped with inorganic acids without any surfactant function can be

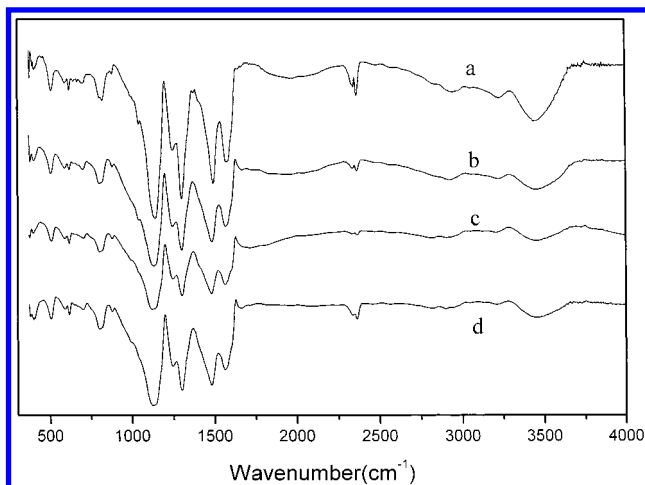


Figure 5. FTIR spectra of PANI nanostructures doped with different inorganic acids: (a) H_2SO_4 , (b) HCl , (c) HBF_4 , (d) H_3PO_4 ($[\text{An}]/[\text{acid}] = 2$, $[\text{SDBS}] = 2.4 \times 10^{-3} \text{ M}$, at $0-4^\circ\text{C}$).

synthesized by a self-assembly process. However, the diameter of PANI nanostructures can be affected through the addition of the surfactant and change in its concentration.

Structural Characterization. The UV-vis spectrum, FTIR spectrum, and X-ray diffraction were used to characterize the molecular structure of the resulting nanostructures of PANI doped with different inorganic acids.

Figure 5 shows the FTIR spectra of PANI-HCl, PANI- H_2SO_4 , PANI- HBF_4 , and PANI- H_3PO_4 nanostructures prepared in the presence of SDBS as a surfactant. It was found that the FTIR spectra of these four PANI were similar. The characteristic peaks at 1567 and 1483 cm^{-1} can be assigned to the stretching vibration of quinoid ring and benzenoid ring, respectively. The bands at 1300 and 1246 cm^{-1} correspond to C-H stretching vibration with aromatic conjugation. These characteristic peaks are identical to those of PANI-(β -NSA) microtubes²⁵ and those of PANI-HCl²⁶ prepared in a common method. The FTIR spectrum of PANI- H_3PO_4 prepared without surfactant is the same as that of PANI- H_3PO_4 prepared with SDBS acting as the surfactant. The results indicate that the backbone structures of PANI-HCl, PANI- H_2SO_4 , PANI- HBF_4 , and PANI- H_3PO_4 nanostructures obtained in this work are identical to each other and also to those of PANI-(β -NSA) microtubes²⁵ and PANI-HCl²⁶ reported previously.

UV-vis spectra of the resulting PANI nanostructures dissolved in *m*-cresol were measured. For all these four PANI nanostructures, two bands at about 430 nm and longer than 850 nm with a long tail are present (Table 1). The peak at longer than 850 nm can be assigned to a polaron band.²⁷ Table 1 shows that the electrical structures of PANI nanostructures are slightly different, depending on the dopants used. However, all these PANI nanostructures are identical to the emeraldine salt form of PANI.²⁸

X-ray scattering patterns of PANI-HCl, PANI- H_2SO_4 , PANI- HBF_4 , and PANI- H_3PO_4 nanostructures are shown in Figure 6. Two broad peaks centered at $2\theta = 20^\circ$ and 26° were observed, showing the resulting PANI nanostructures are amorphous. The peak centered at $2\theta = 20^\circ$ may be ascribed to periodicity parallel to the polymer chain, while the latter peaks may be caused by the periodicity perpendicular to the polymer chain.²⁹

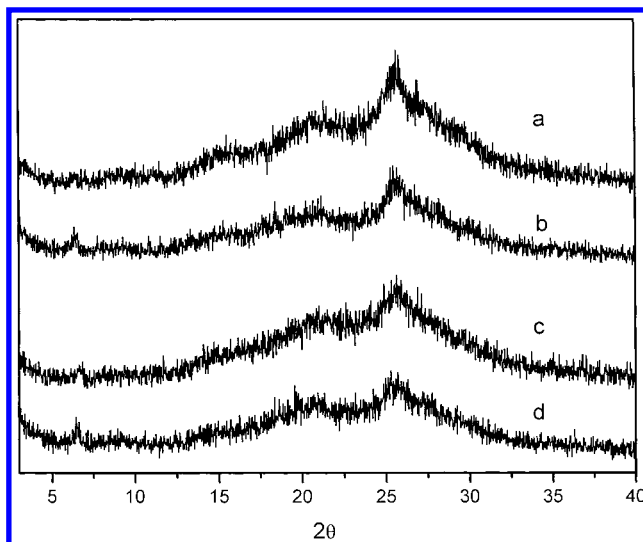


Figure 6. X-ray diffraction of PANI nanostructures doped with different inorganic acids: (a) H_2SO_4 , (b) HCl , (c) HBF_4 , (d) H_3PO_4 ($[\text{An}]/[\text{acid}] = 2$, $[\text{SDBS}] = 2.4 \times 10^{-3} \text{ M}$, at $0-4^\circ\text{C}$).

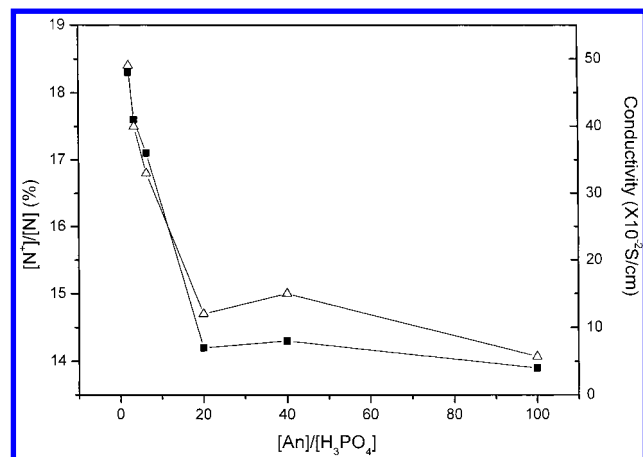


Figure 7. Effect of $[\text{An}]/[\text{H}_3\text{PO}_4]$ on room temperature conductivity and doping degree of PANI nanostructures: Δ , room temperature conductivity; \blacksquare , doping degree ($[\text{An}]/[\text{H}_3\text{PO}_4] = 2$, $[\text{SDBS}] = 2.4 \times 10^{-3} \text{ M}$, at $0-4^\circ\text{C}$).

However, it is noted that the crystallinity of PANI nanostructures doped with inorganic acids is lower than that of PANI-(β -NSA).³⁰ This may be due to different molecular sizes of the dopants or different formation mechanisms of the nanostructures.

Physical Properties. PANI doped with HCl , H_2SO_4 , HBF_4 , and H_3PO_4 has different room-temperature conductivity within the range of $0.49-6.38 \text{ S/cm}$, depending on the dopant used. It was noted that their conductivity were 10–100 times higher than that of PANI nanotubes doped with β -NSA ($\sim 10^{-2} \text{ S/cm}$)³⁰ prepared at an aniline/NSA mole ratio of 1:0.5 ($0-4^\circ\text{C}$). An order of PANI-HCl > PANI- H_2SO_4 > PANI- HBF_4 > PANI- H_3PO_4 in conductivity was observed, and the detailed data are provided in Table 1. The conductivity of PANI- H_2SO_4 and PANI- HBF_4 is consistent with the results of doping degree, assigned as $[\text{N}^+]/[\text{N}]$ measured by XPS. However, the conductivity of PANI-HCl and PANI- H_3PO_4 is not consistent with XPS results (see Table 1). A possible reason may be that the molecular size of H_3PO_4 ,³¹ which is larger than that of HCl , resulted in its lower conductivity. This is consistent with T_0 values as shown in Table 1.

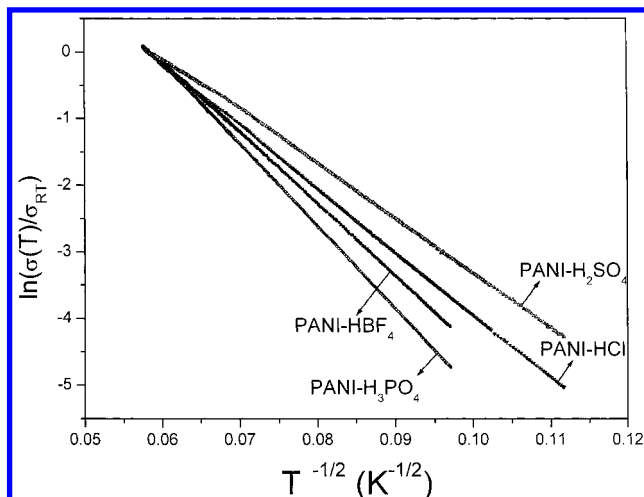


Figure 8. Temperature dependence of conductivity for PANI nanostructures doped with different inorganic acids ([An]/[acid] = 1:0.5, [SDBS] = 2.4×10^{-3} M, at 0–4 °C).

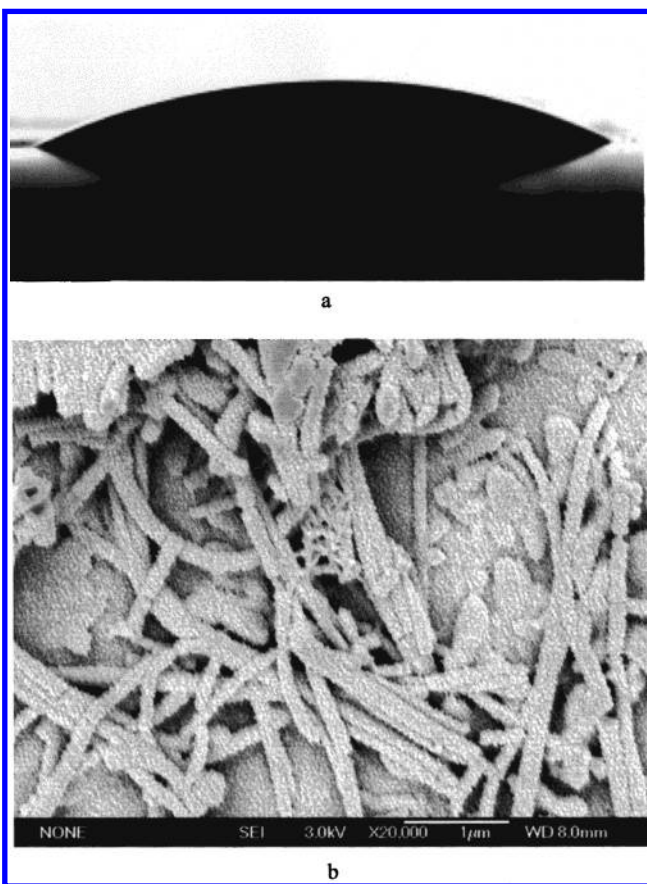


Figure 9. Photograph of water drop on PANI–H₃PO₄ film deposited on the glass substrate (a) and SEM of PANI–H₃PO₄ film (b) ([An]/[acid] = 2, [SDBS] = 2.4×10^{-3} M, at 0–4 °C).

The effect of [An]/[H₃PO₄] on the conductivity of PANI–H₃PO₄ nanostructures was measured. However, there was no significant difference in conductivity, around 10^{-2} S/cm, when [An]/[H₃PO₄] varied from 1:0.5 to $1:2.5 \times 10^{-2}$. As the aniline/H₃PO₄ mole ratio reached $1:1.0 \times 10^{-3}$, the conductivity decreased to 5.7×10^{-2} S/cm. This result is consistent with the doping degree as shown in Figure 7.

The temperature dependence of conductivity of PANI doped with different inorganic acids was measured

between 50 and 300 K. It was found that the conductivity of all measured samples decreased with decreasing temperature, exhibiting a typical semiconductor behavior. The data are best fit to the relationship of $\ln \sigma$ plotted vs $T^{-1/2}$ as shown in Figure 8. So it is reasonable to believe that the temperature dependence of conductivity of all these PANI nanostructures is in agreement with one-dimensional variable range hopping (1D-VRH) model proposed by Mott,³² which is expressed as

$$\sigma(T) = \sigma_0 \exp[-(T_0/T)^{1/n+1}], \quad n = 1, 2, 3$$

where σ_0 is a constant, T_0 the hopping barrier, and T the Kelvin temperature. The T_0 values of PANI nanostructures doped with different acids are comparable to those reported in the literature.³³ The T_0 value follows an order of PANI–H₃PO₄ > PANI–HBF₄ > PANI–H₂SO₄ > PANI–HCl, which is consistent with a trend of their room-temperature conductivity.

Interestingly, it was found that PANI–H₃PO₄ nanostructural films deposited on the glass substrate exhibited hydrophilic behavior, which was confirmed by measuring contact angle with water ($\theta = 32^\circ$). Figure 9 shows the photograph of water drop on PANI–H₃PO₄ film (a) and SEM of PANI–H₃PO₄ nanostructure film (b). Similarly, PANI–HCl, PANI–H₂SO₄, and PANI–HBF₄ films all are hydrophilic, and their contact angles with water are 40° , 38° , and 27° , respectively.

Conclusions

Nanostructures (e.g., nanotubes or nanorods) of PANI doped with HCl, H₂SO₄, HBF₄, and H₃PO₄ with an average diameter of 150–340 nm and a conductivity of 10^{-1} – 10^0 S/cm were synthesized in a self-assembly method with and without a surfactant. It was found that the morphology, size, room-temperature conductivity, and T_0 value of the nanostructures depended on the dopant structures and reaction conditions. In particular, lower reaction temperature (e.g., 0–4 °C) and some [An]/[acid] ratio values (1:0.5, 1:0.3, and 1:0.16) were favorable to the formation of PANI nanostructures. In the presence of a surfactant, micelles formed by anilinium cations and surfactant anions were regarded as templates in the formation of the nanostructures. In the absence of a surfactant, on the other hand, micelles formed by anilinium cations were considered as templates. However, the size of PANI nanostructures was slightly affected by the addition of the surfactant during the polymerization. Interestingly, the resulting PANI nanostructural films show hydrophilic behaviors, and the contact angles with water depend on the dopant used. FTIR and UV–vis spectra, XPS, and X-ray diffraction measurements show that the main chain structure and electrical structure of PANI nanostructures are identical to those of the emeraldine salt form of PANI. Moreover, the resulting nanostructures are also amorphous, similar to granular PANI doped with inorganic acids.

Acknowledgment. This project was supported by the National Natural Science Foundation of China (No. 29974037, 50133010), 973 Program of China (No. G1999064504), and Center of Molecular Sciences, Institute of Chemistry, Chinese Academy of Sciences (No. CMX-CX 2001). The authors thank Prof. Zhaojia Chen and Mr. Yunze Long for measuring σ – T curves.

References and Notes

- (1) Iijima, S. *Nature (London)* **1991**, 354, 56.
- (2) Cao, Y.; Smith, P.; Heeger, A. J. *Synth. Met.* **1992**, 48, 91.
- (3) Martin, C. R. *Science* **1994**, 266, 1961.
- (4) Liang, W.; Martin, C. R. *J. Am. Chem. Soc.* **1990**, 112, 8976.
- (5) Cai, Z.; Martin, C. R. *J. Am. Chem. Soc.* **1989**, 111, 4138.
- (6) Martin, C. R. *Adv. Mater.* **1991**, 3, 457.
- (7) Cai, Z.; Lei, J.; Liang, W.; Menon, V.; Martin, C. R. *Chem. Mater.* **1990**, 3, 960.
- (8) Wan, M. X.; Shen, Y. Q.; Huang, J. Chinese patent No. 98109916.5, 1998.
- (9) Huang, J.; Wan, M. X. *J. Polym. Sci., Part A: Polym. Chem.* **1999**, 37, 151.
- (10) Liu, J.; Wan, M. X. *J. Mater. Chem.* **2001**, 11, 404.
- (11) Liu, J.; Wan, M. X. *J. Polym. Sci., Part A: Polym. Chem.* **2001**, 39, 997.
- (12) Wan, M. X.; Huang, J.; Shen, Y. Q. *Synth. Met.* **1999**, 101, 708.
- (13) Shen, Y. Q.; Wan, M. X. *J. Polym. Sci., Part A: Polym. Chem.* **1999**, 37, 1443.
- (14) Wan, M. X.; Li, J. C. *J. Polym. Sci., Part A: Polym. Chem.* **1999**, 37, 4605.
- (15) Wan, M. X.; Liu, J.; Qiu, H. J.; Li, J. C. *Synth. Met.* **2001**, 119, 71.
- (16) Qiu, H. J.; Wan, M. X.; Matthews, B.; Dai, L. M. *Macromolecules* **2001**, 34, 675.
- (17) Qiu, H. J.; Wan, M. X. *Chinese J. Polym. Sci.* **2001**, 19, 65.
- (18) Yang, Y. S.; Wan, M. X. *J. Mater. Chem.*, in press.
- (19) Wan, M. X.; Li, J. C. *J. Polym. Sci., Part A: Polym. Chem.* **2000**, 38, 2359.
- (20) Funrhop, J. H.; Helfrich, W. *Chem. Rev.* **1993**, 93, 1565.
- (21) Elia, H. G. In *Macromolecules 2, Synthesis and Materials*; Plenum Press: New York, 1977; p 73.
- (22) Kim, B. J.; Oh, S. G.; Han, M. G.; Im, S. S. *Synth. Met.* **2001**, 122, 297.
- (23) Kim, B. J.; Oh, S. G.; Han, M. G.; Im, S. S. *Langmuir* **2000**, 16, 5841.
- (24) Harada, M.; Adachi, M. *Adv. Mater.* **2000**, 12, 839.
- (25) Huang, J.; Wan, M. X. *J. Polym. Sci., Part A: Polym. Chem.* **1999**, 37, 151.
- (26) MacDiarmid, A. G.; Chiang, J. C.; Halpern, M.; Huang, W. S. *Mol. Cryst. Liq. Cryst.* **1985**, 121, 173.
- (27) MacDiarmid, A. G.; Epstein, A. J. *Synth. Met.* **1994**, 65, 103.
- (28) Cao Y.; Smith, P.; Heeger, A. J. *Synth. Met.* **1989**, 32, 236.
- (29) Moon, Y. B.; Cao, Y.; Smith, P.; Heeger, A. J. *Polym. Commun.* **1989**, 30, 196.
- (30) Zhang, Z. M.; Wan, M. X. *Synth. Met.*, in press.
- (31) The P–O band length was calculated by the software: SymApps 5.0 written by Karl Nedwed, Copyright-1997 Bio-Rad Laboratories.
- (32) Mott, N. F.; Davis, E. A. *Electronic Processes in Non-crystalline Materials*, 2nd ed.; Clarendon Press: Oxford, 1979; p 34.
- (33) Kobayashi, A.; Xu, X.; Ishikawa, H.; Satch, M. *J. Appl. Phys.* **1972**, 5702.

MA020199V